JOURNAL OF SPACECRAFT AND ROCKETS
Vol. 31, No. 2, March–April 1994

Analysis of Multifastener Composite Joints

O. H. Griffin Jr.* and M. W. Hyer†
Virginia Polytechnic Institute and State University, Blacksburg, Virginia 24061
D. Cohen‡
Hercules Aerospace Company, Magna, Utah 84044
M. J. Shuart§
NASA Langley Research Center, Hampton, Virginia 23681
S. R. Yalamanchili¶
General Motors Truck Engineering, Warren, Michigan 48091
and
C. B. Prasad**
Analytical Services and Materials, Inc., Hampton, Virginia 23666

A new numerical procedure for determining load proportioning in multifastener mechanical joints in composite plates is presented. The joints are loaded in double lap fashion in tension with pins through the holes. The commercial finite element program ABAQUS is used to predict the load proportioning among fasteners using two independent plane stress finite element models, one representing the composite inner lap and one representing the two steel outer laps, interacting through rigid circular surfaces. The circular surfaces effectively represent rigid pins. Load proportioning is predicted for a number of geometries. Excellent correlation with experimental data is obtained. Experimental and computed surface strains are also found to compare well. The assumption of a radial cosine distribution of contact stress between fastener and hole boundary, often used in these studies, is shown to be substantially in error for some holes.

Introduction

SOME composite solid rocket motor case designs call for the joining of two or more large cylindrical sections end to end. The exact details of the joint design depend on the application, but all of the joints have several characteristics in common. One characteristic is that heavily loaded circumferential joints are designed using mechanical attachments. A pattern of drilled holes is specified for the joint, as illustrated in Fig. 1, to accommodate the fasteners, which may be bolts or pins. The number of holes and the specific hole pattern is dependent on the exact application, but generally more than one row of holes is required for an effective design. The pattern shown in Fig. 1 has two rows: the row closest to the end being referred to as the outboard row and the row away from the end being referred to as the inboard row. Also, the two rows shown in Fig. 1 are circumferentially staggered relative to one another, as is common for joint designs.

The analysis and testing of any joining configuration is an immense and extremely expensive task. If interest is focused on the design of a joint to resist tensile loads, say, in pulling the cylinders apart axially, full-scale testing may simply be impossible. One solution to this problem is the testing, and companion analysis, of segments of the cylinder, say, the slice shown by the blowup in Fig. 1. The analysis of segments immediately raises the issue of how wide to make the segment, i.e., how many fasteners, to properly represent the large number of fasteners in the actual cylinder. In addition to the question of segment width, the curvature of a cylindrical segment presents challenging experimental problems. With the staggered rows of Fig. 1, the additional question of the effects of the partial holes on specimen response and subsequent translation to joint design information must be addressed. This paper discusses the results of a multifaceted program aimed at understanding the mechanical joining of cylinders. Specifically, the discussion focuses on the testing and analysis of a series of multifastener joint specimens. Because of the complications associated with testing of curved segments, this initial work is restricted to flat geometries. Reported herein is the analysis of the multifastener joints and, to the degree to which they validate the

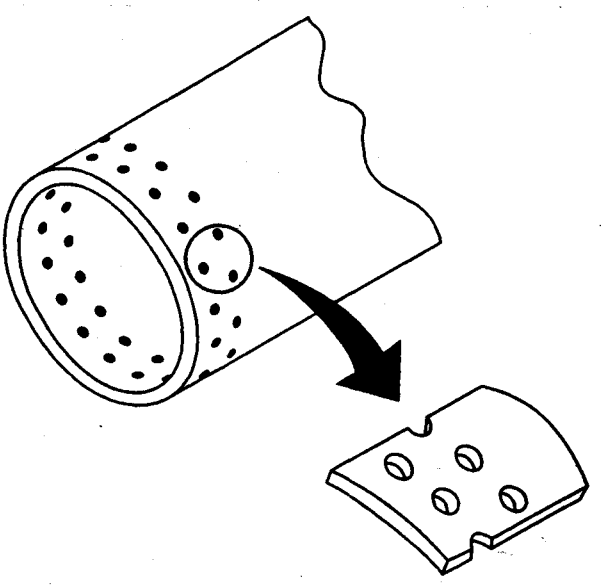

Fig. 1 Schematic of cylinder drilled for mechanical joining.

Received May 21, 1992; revision received March 20, 1993; accepted for publication March 22, 1993.

*Associate Professor, Department of Engineering Science and Mechanics. Senior Member AIAA.
†Professor, Department of Engineering Science and Mechanics. Associate Fellow AIAA.
‡Research Engineer, Bacchus Works, P.O. Box 98/MS N2EA16. Senior Member AIAA.
§Assistant Chief, Structural Mechanics Division. Senior Member AIAA.
¶Senior Project Engineer, Engineering Analysis, 2500 E. Nine Mile Road.
**Research Engineer, 107 Research Drive. Member AIAA.

analysis, some of the experimental results. It is important to note that there have been numerous studies which have had as their focus the joining of composite structures. Early work considered single-fastener joints,[1,2] although multiple fastener joints were certainly of interest.[3,4] Work continued in both single- and multiple-fastener joints,[5,6] with there being particular interest in the influence of friction, clearance, and fastener elasticity[7]; nonlinear material effects[8]; proportioning of load among fasteners[9]; and bypass loads.[10] However, because of the complexity of the joints studied and the approached used, the present study is believed to be unique.

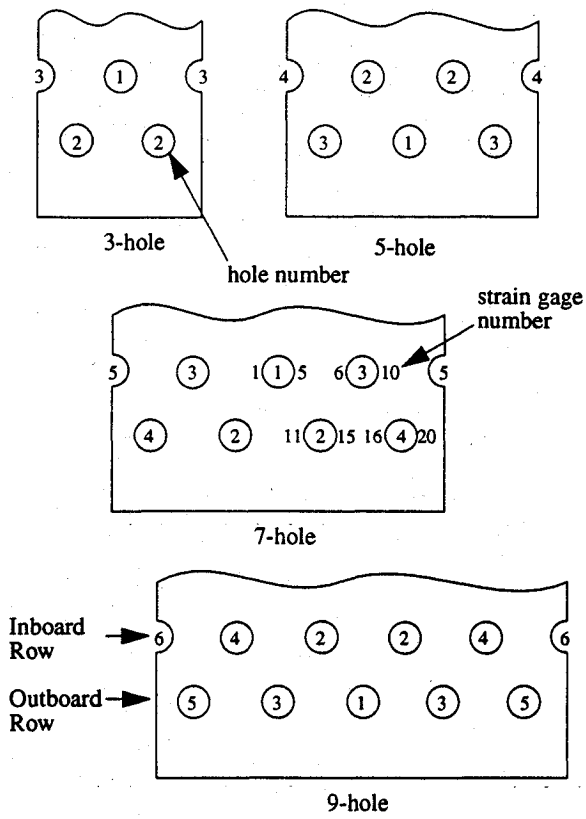

Fig. 2 Schematic of specimens tested and analyzed, showing hole and strain gauge numbering.

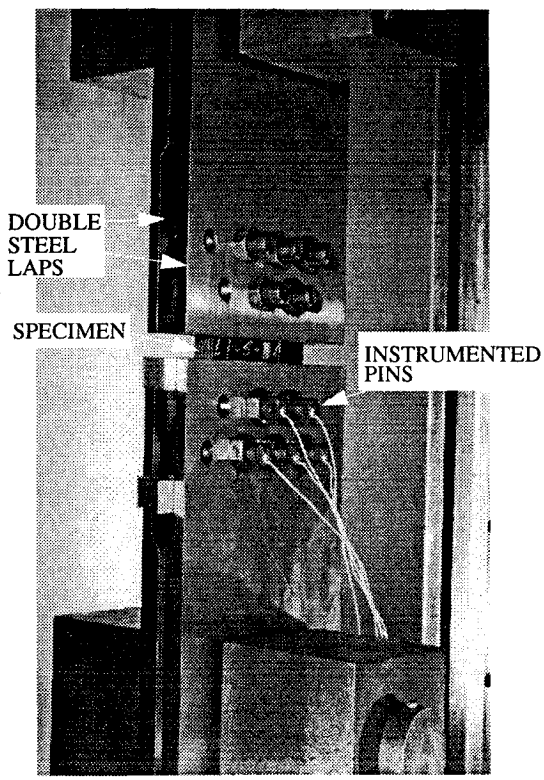

Fig. 3 Photograph of test setup.

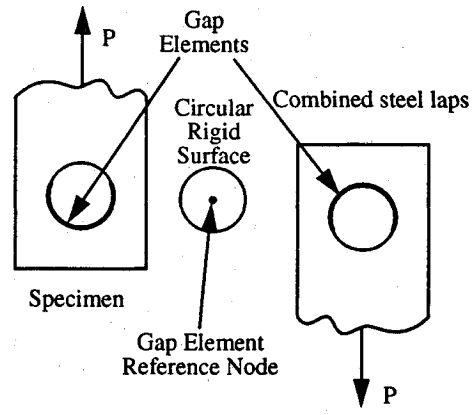

Fig. 4 Components of finite element model.

Geometries Studied

To begin to address the issues associated with the analysis and testing of segments of cylinders, multifastener specimens of various widths were fabricated. One family of the specimen geometries is shown in Fig. 2, the specimens being referred to as 3-, 5-, 7-, and 9-hole specimens, corresponding to the number of loaded holes in each end of the specimen. In Fig. 2 the holes are numbered, hole 1 being on the centerline, etc., and the locations of strain gauges at the net section hole edges of the 7-hole specimen are indicated. Note that with these geometries the unloaded half-hole is always in the inboard row. Specimens with 5 and 7 holes per end and the unloaded half-holes in the outboard row were also tested and analyzed but are not discussed herein. The material system chosen for the effort is IM7G/3501-6. The specimens are approximately 1 in. thick, and the holes are 0.75 in. in diameter. In a given row the hole centers are 1.875 in. apart, and the two rows are axially separated by 1.5 in. The hole centers in one row are circumferentially offset with respect to the hole centers in the other row by half of the hole spacing, as shown in Fig. 2. The distance from the centers of the outboard holes to the end of the specimen is 1.75 in. for all of the cases. The overall axial length of the specimens is 10.25 in. The widths are 3.75 in. for the 3-hole specimens, 5.625 in. for the 5-hole specimens, 7.5 in. for the 7-hole specimens, and 9.375 in. for the 9-hole specimens. Although three different lamination sequences were tested and analyzed during the course of this study, only one, $\{[(\pm 15)_3/90_2/0/(\pm 45/0)_5/90_3]_6/(\pm 15)_3\}_T$, will be reported herein. The specimens were manufactured and machined to specification by Hercules Aerospace, Inc.

Experiments

Test specimens were loaded in uniaxial tension using a 1200-kips capacity hydraulic testing machine at NASA Langley Research Center. The loaded ends of the specimens were fastened between steel fixtures (laps) with hardened steel bolts to form a double-lap configuration. The double steel laps totaled 1 in. in thickness in the joint but were tapered to approximately twice that thickness away from the joint. The bolts were not torqued and hence acted as pins, exerting no through-the-thickness force on the joint. Thus, the so-called clamp-up effect was not a factor, although it might be in some applications. A typical specimen (5-hole specimen, unloaded half-hole in the inboard row) in the testing machine is shown in Fig. 3. The load was applied slowly to simulate a static loading condition. Needless to say, the 7- and 9-hole specimens required considerable force P to cause failure. Specially instrumented pins[11] were used to determine the percentage of load reacted by each fastener. Electrical resistance strain

gauges (nominal gauge length 0.070 in., nominal width 0.022 in.) were used to monitor specimen strains around the holes and elsewhere on the specimen. Electrical signals from the instrumentation and the corresponding applied loads were recorded at regular time intervals during the test. More strain gauges were used in the experiments than are shown in Fig. 2 but are not reported herein, since they were not used specifically for verification of the analyses.

Analysis

In addition to the experiments, finite element analyses were performed to determine the response of the different joint geometries. With these specimens there were the issues of 1) knowing what percentage of the total load is reacted by each fastener, 2) knowing how the fastener interacts with the hole boundary, and 3) knowing the strains within the composite, particularly around the hole. The answer to the first question is directly related to the compliance of the steel laps and the compliance of the composite specimens. The latter issues, however, in addition to depending on the specimen and lap compliances, also depend on fastener-hole clearance, friction, fastener compliance, and several other factors.

To model the loading of the specimens, the finite element program ABAQUS (version 4.8)[12] was used. Because the compliance of the steel laps is so important in determining the percentage of load reacted by each fastener, both the composite specimen and the steel laps were modeled. A state of plane stress was assumed, so the analyses were two dimensional. Furthermore, since the joints were double lapped, and thus introduced no out-of-plane bending into the system, the two steel laps were modeled as a single lap with the appropriate thickness. The independent (no common nodes or degrees of freedom) steel lap and composite specimen finite element models were made to interact through rigid circular surfaces with centers initially at the centers of the holes. The different components of the finite element model of the joints are shown schematically in Fig. 4. Note that in the finite element model the centerplanes of the two plane stress models are actually coplanar. The rigid circles that represent the fasteners in the joint interact with the elastic composite and steel components through gap (ABAQUS IRS22 for the present analyses) elements, which have no spatial dimensions and are "paved" onto the faces of the finite element model where contact is anticipated, as shown in Fig. 4. These gap elements, which were on both the steel and composite, are mathematically prevented from crossing the boundaries of the associated rigid circular surfaces. To make the two independent finite element models interact, the IRS22 elements associated with the composite specimen and the IRS22 elements associated with the steel lap for a particular hole were referenced to the same nodal point, which was placed at the hole center. Note that these rigid surface reference nodes were not connected to any finite elements in the standard sense, only to the rigid surfaces. Unless they were located on symmetry lines, the nodes at the centers of those circles were free to move in the plane of the specimen and lap and were thus able to represent movement of one fastener center relative to the others due to the different compliances of the steel and composite. Neither friction nor hole clearance was modeled, but with care in the experiments, the latter would not be an issue, and previous studies indicate that although the inclusion of friction and fastener compliance can influence the predicted stresses, they are not first-order effects.[7]

Both of the components (composite and steel) were modeled as linear elastic solids. The composite was assumed to have orthotropic properties (type = lamina in ABAQUS), and the steel was assumed to be isotropic. Both components were modeled with 8-node two-dimensional plane stress elements (CPS8). The material properties used for IM7G/3501-6 were $E_1 = 29.4$ Msi, $E_2 = 1.01$ Msi, $\nu_{12} = 0.26$, and $G_{12} = 0.764$ Msi, and for steel were $E = 30$ Msi and $\nu = 0.3$. The inplane elastic constants of the laminate were computed from classical laminated plate theory, resulting in laminate properties for the just mentioned stacking sequence of $E_x = 12.48$ Msi, $E_y = 6.97$ Msi, $\nu_{yx} = 0.191$, and $G_{xy} = 3.05$ Msi (where the x axis coincides with the loading direction). Whereas the laminates used in the experiments were nonsymmetric, examination of the coupling matrix $[B]$ indicated that the bending-stretching coupling terms were small for this 168-ply laminate. Therefore, it was

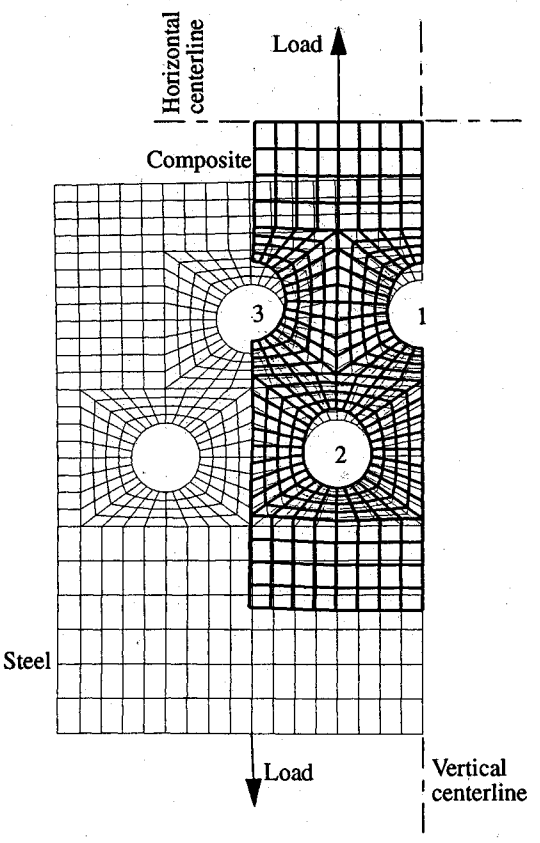

Fig. 5 Deformed finite element model of 3-hole specimen and steel lap.

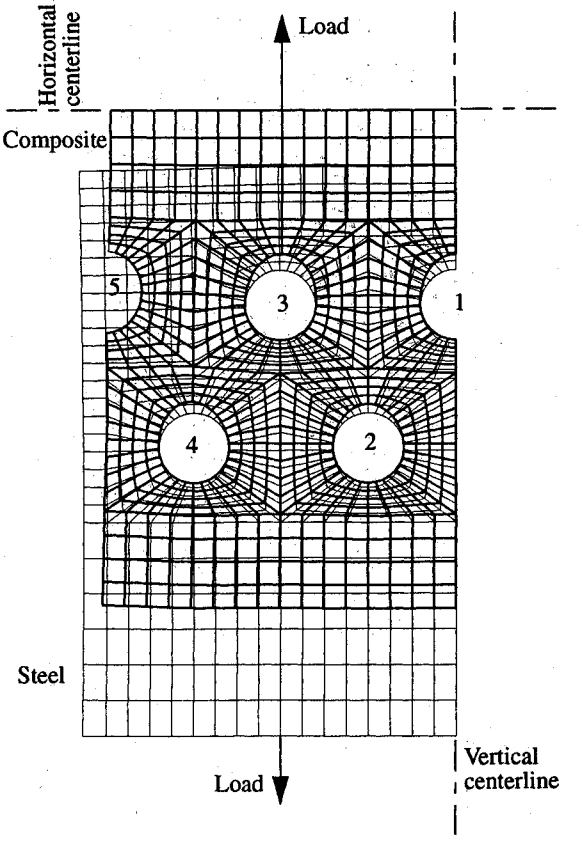

Fig. 6 Deformed finite element model of 7-hole specimen and steel lap.

Table 1 Percent of load reacted by each fastener

	Hole 1[a]		Hole 2		Hole 3		Hole 4		Hole 5	
Specimen	Num[b]	Exp	Num	Exp	Num	Exp	Num	Exp	Num	Exp
3 hole	41	38	30	32						
5 hole	13	14	24	24	20	19				
7 hole	15	15	10	12	18	16	15	15		
9 hole	8	8	12	13	8	8	14	13	12	12

[a]Each specimen has a single hole 1, but other holes occur in pairs.
[b]Numerically (Num) computed percentages, as well as experimental (Exp) percentages, may not add to 100.

assumed that induced out-of-plane bending due to coupling was small and thus was ignored.

The deformed finite element models of the 3- and 7-hole composite specimens (darker lines) and steel laps (lighter lines) are illustrated in Figs. 5 and 6, respectively. As can be seen, only the lower left quadrant of a left-right, up-down symmetric model was considered. (A single set of steel laps was used to test the 3- and 7-hole specimens, and another set was used to test the 5- and 9-hole specimens. Hence the steel laps were considerably wider than the 3- and 5-hole specimens. However, since the testing was done in this fashion, the numerical modeling included this effect.) Nodes on the vertical centerline, including the rigid surface reference node for hole 1, were constrained to move only vertically. Nodes on the horizontal centerline were constrained to have equal vertical displacements, with no constraint on their horizontal displacements except at the vertical centerline. These constraints, essential to proper modeling of the horizontal symmetry line, were accomplished using multipoint constraints. Thus the Poisson width contraction of the specimen was only suppressed by its interaction with the steel lap. Nodes on the bottom edge of the steel lap were constrained to have no displacement, since that corresponds to the location where the thickness of the steel lap doubles. The double thickness (2-in.-thick) steel was considered to be rigid for the present analyses. A single vertical point load equal to the desired load on the model was then applied at a nodal point on the horizontal centerline.

The 3-hole model (Fig. 5) is unique in the current set of analyses in that it has very few fasteners, resulting in the single inboard centerline fastener carrying a very large portion of the load, as will be discussed in more detail later. Hole 1 in the model is the inboard centerline hole, and hole 3 is an unloaded half-hole (see Fig. 2). A quick glance at the deformed finite element model of Fig. 5 reveals some of the distortions resulting from the loading. First, note that the space occupied by the rigid circular fasteners is preserved. Also, all of the holes in the composite are elongated. In addition, hole 2 tends to elongate considerably in the direction of hole 3, as opposed to distorting in the loading direction. This skewing of outboard row holes in the direction of unloaded inboard row half-holes was found to be characteristic of these specimens. The unloaded half-hole (3) acts as a semicircular notch and distorts severely. Finally, the gapping (opening of space between the hole edge and fastener on the unloaded side of the fastener) between the steel and the rigid surface is seen to be smaller than the gapping between the composite and the rigid surface for a given hole. This is due to the substantially larger modulus of the steel (30 Msi for steel compared to 12.48 Msi for the composite). Gapping between fastener and specimen is also seen to be considerably larger for hole 1 than for hole 2, giving a qualitative indication that the fastener in hole 1 is carrying more load than the fastener in hole 2. This will be shown quantitatively later.

The deformed mesh of the 7-hole joint, Fig. 6, shows some similarity to the 3-hole model, although qualitatively (by comparison of gapping between specimen and fastener for different holes) it appears that the load is much more evenly distributed in the 7-hole joint than for the 3-hole joint. There does appear, however, to be some inequality in load proportioning based on unequal gapping at all of the holes. There is considerably less skewing of the outboard holes in the specimen toward the unloaded half-hole (5), and the distortion in the unloaded half-hole is smaller than in the 3-hole joint. Again, note that the gapping between the steel and the rigid surface is smaller than the gapping between the composite and the rigid surface for a given hole. As expected, and verified by comparison of Figs. 5 and 6, there is considerable difference in the details of the response of narrow and wide specimens.

Experimental/Numerical Correlation

Physically, the steel lap/fastener and specimen/fastener interactions are load-level dependent and result in distortion of the joint components. The resulting contact problem must be solved incrementally, with some iteration at each load step. Not only do the holes elongate, but there is a sliding of the hole surface around the fastener in the direction of load. After the final load step, the percentage of load reacted by the fastener in a particular hole can be determined by integrating the stresses on the boundary of that hole and resolving them to find the load-direction component. Also, the distribution of stresses around the hole can be determined. These stress distributions can be used in equivalent single-lap models if desired. During the course of this work, it was found that the two-mesh model being described here runs quite efficiently, and hence there is really no need for equivalent single-lap models.

Previously, a common practice was to assume an interaction between fastener and hole which resulted in a circumferential distribution of normal contact stress which varies as the cosine of the angle from the bottom of the hole, normally under the additional assumption that each fastener reacts the same percentage of the total load, or possibly that each row of fasteners reacts an equal portion of the total load. With the model being described here, the validity of this approach can be determined.

A comparison between the experimentally measured and numerically predicted load proportioning among the fasteners for the 3-, 5-, 7-, and 9-hole specimens is given in Table 1. The experimental values for the off-centerline fasteners were computed by averaging the values (which were not always equal) for a pair of fasteners symmetrically placed with respect to the centerline. The numerical load proportions were calculated by numerically integrating the load-direction components of the interference stresses reported by the ABAQUS interface elements. The computation was done at loads equal to 50 and 75% of the experimental failure loads for the corresponding specimen. Numerically, it was found that load proportions were not substantially affected by the level of applied load, and that the proportions at the two load values were essentially equal. As can be seen from Table 1, the comparison between analysis and experiments is quite good, with the maximum difference occurring at fastener 1 of the 3-hole specimen, and being only 3% of the applied load in that case. To assess the viability of this approach as a design tool for mechanical joints in composites, the relatively low computational cost of these runs (1000–1500 CPUs on an IBM 3090, nonvectorized) and the good comparison with experiments prompted additional comparisons.

Note in Table 1 that the discussed qualitative assessment (from examination of the deformed finite element models) of larger load in the fastener in hole 1 of the 3-hole specimen than for the fastener in hole 2 is supported by both the numerically integrated stresses and the experimental values. The centerline fastener in the 3-hole specimen carries approximately 40% of the total load, with only 30% carried by each of the other two fasteners. As the number of fasteners increases, the load proportioning becomes more equal. The smaller imbalance previously indicated qualitatively by examination of the deformed finite element model of the 7-hole specimen is also indicated by the values in the table. The 9-hole speci-

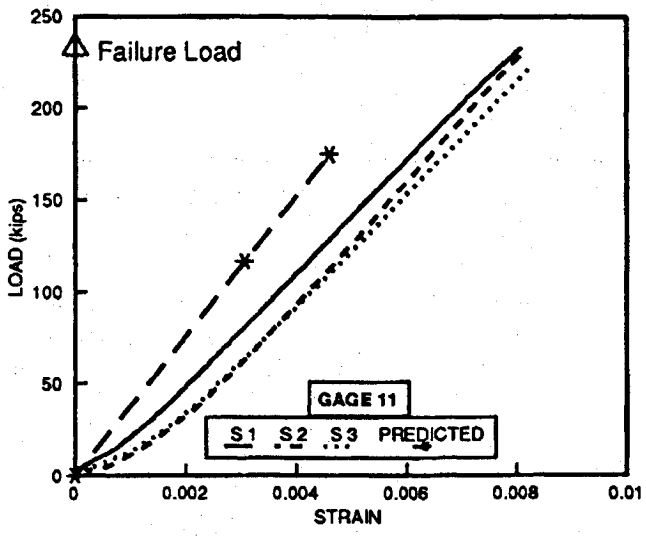

Fig. 7a Comparison of predicted and measured strains, 7-hole specimen, gauge 11.

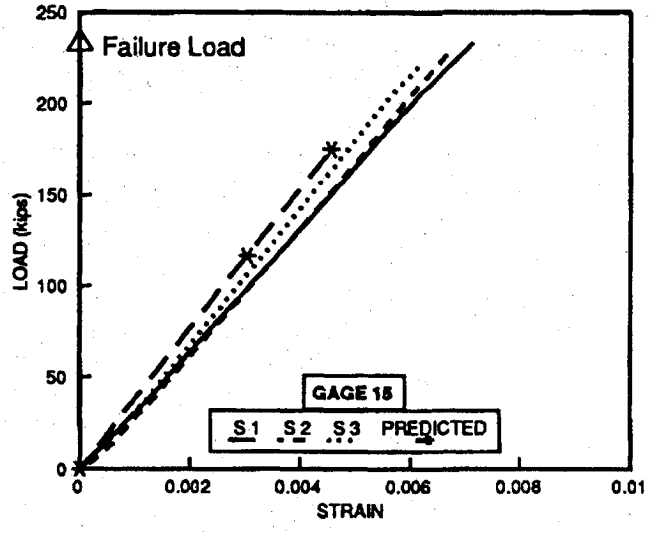

Fig. 7b Comparison of predicted and measured strains, 7-hole specimen, gauge 15.

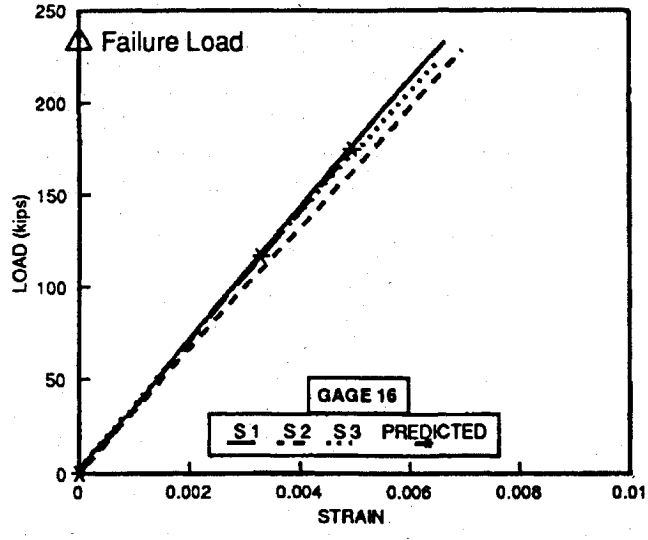

Fig. 7c Comparison of predicted and measured strains, 7-hole specimen, gauge 16.

men shows even smaller imbalance in load proportioning and approaches the experimental values previously reported by Cohen et al.[11] for similar multifastener mechanical joints in composites. Their data indicated that assuming 50% of the load was carried by each row of fasteners was reasonable. Comparison of the percentage of total load carried by each row of fasteners for the experiments and analysis can be accomplished from the data in Table 1. It can be seen that the outboard row carries a substantially larger portion of the load in narrower specimens, with a shift to the inboard row carrying a slightly larger portion in the wider specimens. This is, however, somewhat misleading for the 3-hole specimen, in which the single fastener in the inboard row carries 40% of the total load.

Unfortunately, it has not been possible to experimentally verify one of the more interesting results of the finite element analyses, the predicted skewing of hole elongation in the direction of the unloaded half-holes. Experimental verification has not been possible because the specimens are almost completely obscured by the steel laps, as shown in Fig. 3.

As another comparison between the experiments and analyses, the experimentally determined strains at some of the net section hole edges for a 7-hole specimen are shown in Figs. 7a–7c. The gauge numbering was shown with the 7-hole specimen in Fig. 2. There were three replicate specimens, denoted as S1, S2, and S3. The strain responses of the three specimens are shown. Finite element calculations were obtained for two load levels, corresponding to 50 and 75% of the experimental failure load of the particular specimen, the levels being indicated by the asterisks. The actual failure load of the 7-hole specimen, as determined by the average of two of the three replicate tests, is indicated in the figures. The third specimen was loaded to 95% of the average failure load of the first two and then unloaded for x-ray analysis. Despite the problem being one of contact, the numerically predicted load vs strain relationships were practically linear. Thus, extrapolation to predictions at higher loads appears to be straightforward. As can be seen, there is good correlation between the experiment and prediction for the majority of the gauges. Good comparison was also achieved for the gauges not presented here. The comparisons presented in Figs. 7a–7c are representative. It should also be noted that the relatively poor comparison of Fig. 7a is largely due to a difference in slope during the initial loading. After the load increases slightly, the slopes of the experimental and numerical curves are very similar. The lack of correlation that does exist, such as for gauge 11, is attributed to the lack of initial alignment, slightly unequal hole sizes, and other anomalies in the experiments.

Fastener-Hole Interaction

Also of interest is the manner in which the composite specimen interacts with the rigid fasteners. Accurate prediction of the distribution of contact stress around the hole is mandatory if accurate predictions of failure load and mode are to be achieved. The standard approach for a particular fastener, given the load proportion, and thus the axial loading, would be to assume that the normal contact stresses vary as the cosine of the angle measured from the bottom of the hole and compute the local stresses from that distribution. Failure predictions would then be based on these local stresses and some criterion. The results of the present finite element analyses allow the validity of that procedure to be checked.

The computed distributions of radial contact stress σ_r around the holes in the 3- and 7-hole specimens ($\theta = 0$ deg is at the bottom of the hole) are shown in Figs. 8 and 9, respectively. The contact stresses are normalized by the average computed bearing stress σ_b. (The quantity $\sigma_b = P/dt$, where P is the computed axial force borne by the boundary of a particular hole, d the hole diameter, and t the specimen thickness.) It should be noted that the distributions shown in those figures were computed both directly from the ABAQUS interface element results and also by integrating and resolving the radial stresses at the Gauss points nearest the hole surface in the composite specimens, with nearly identical results.

Examination of the circumferential distributions of radial contact stress reveals a number of interesting features. The distribu-

tions for some of the hole boundaries appear to be approximately cosinusoidal, but others are definitely not. The distributions for the hole boundaries in the inboard row of all specimens exhibit lower contact stresses at the bottom of the hole than at angular positions substantially away from the bottom.

Examination of the circumferential contact stress distributions for a number of analyses, both of inboard unloaded half-hole and outboard unloaded half-hole specimens, with both isotropic materials and a number of different sets of composite properties, indicates that loaded inboard row holes that are straddled by loaded outboard row holes exhibit a circumferential distribution of contact stress that is definitely not cosinusoidal but has lower contact stress at the bottom of the hole than at angular positions substantially away from that location. The converse is also true; that is, loaded inboard row holes that are not straddled by loaded outboard row holes (does not occur for the geometries reported herein, but does occur in specimens with outboard half-holes) exhibit distributions that are somewhat cosinusoidal. Loaded outboard row holes always exhibit distributions that are somewhat cosinusoidal. Note, however, that these distributions may be skewed relative to the $\theta = 0$ deg (vertical) position, corresponding to the just mentioned skewed elongation of the holes in the direction of the unloaded half-hole. This is particularly noticeable for hole 2 of the 3-hole specimen, Fig. 8. It is believed that the load path in these specimens, especially as affected by the unloaded half-hole, results in these unexpected contact stress distributions.

Given the good correlation of experimental and numerical load proportion and strain data that has been achieved, a high level of confidence has been developed in computing both the load proportioning between the various fasteners in the mechanical joints and the strains. The next step would be to compute the individual layer stresses, based on the computed strains, which have been validated by the experiments. These strains and/or stresses can then be used either in a failure criterion to evaluate the performance of a given design or possibly to choose or develop a failure criterion for this complicated problem.

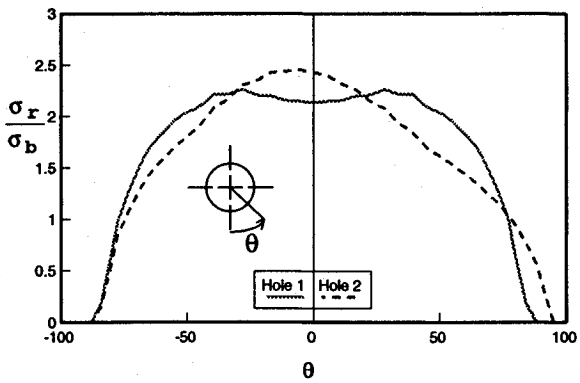

Fig. 8 Contact stress distribution around holes in 3-hole specimen.

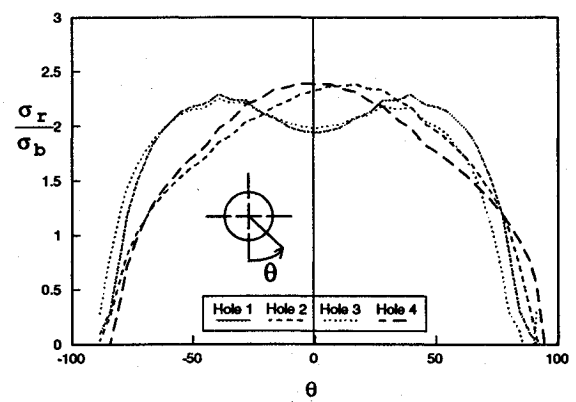

Fig. 9 Contact stress distribution around holes in 7-hole specimen.

Concluding Comments and Contributions

This paper discusses a methodology, not previously used, for understanding and predicting the response of multifastener composite joints. The use of independent, but interacting, finite element models for the steel laps and the composite specimen is unique, and the approach can be applied to a number of other problems, e.g., three rows of fasteners. The method is general enough to be used in design studies of mechanical joining configurations. Because it has been demonstrated with a commercially available finite element software package, the methodology is generally available. Some additional detail is available in Ref. 13.

The model, which includes two finite element meshes interacting through rigid cylindrical surfaces representing the fasteners, is a viable approach to the problem. The geometry and compliances of the steel and composite, and their interactions, are accurately reflected with such an analysis. Computationally, the runs are quite economical.

There is good correlation between the modeling and the experimental results with regard to determination of the percentage of total load carried by each fastener in a multifastener (specifically, multifastener, multirow) mechanical joint. Computed net section strains also agree well between the models and experiments. The complex nature of the load paths in such specimens is revealed by examination of deformed finite element grids, which indicate considerable skewing in the elongation of some loaded holes, usually in the direction of the unloaded half-hole in the current specimens.

It was found that the commonly assumed radial cosine contact stress distribution between the fastener and composite is quite inaccurate for some holes and somewhat accurate for others, even in the same specimen. It appears that load path effects in multirow mechanical joints are responsible for substantial deviations from this commonly assumed distribution.

Load proportioning between rows of fasteners in mechanical joints is seen to be strongly influenced by the number of fasteners. For narrow specimens, that may have few fasteners in a given row, individual fasteners may be extremely heavily loaded. If failure is related to effects which occur around or near holes, as is expected, the narrow specimens may not be very useful in prediction of the behavior of wide or continuous (as is the case for cylindrical sections) joints.

In the joints analyzed, load proportioning was not strongly influenced by load magnitude. During the nonlinear finite element analyses, it was noted that once the first few percent of the total load was applied and converged, the solution proceeded rapidly. Experimentally, load proportion was not substantially affected by load until local failures occurred in the composite specimens.

The approach developed and verified during this study appears suitable as a design tool for mechanical joints in composites. The approach obviates the need to make a number of rather common assumptions, such as the proportioning of total load between individual fasteners or rows of fasteners, or that the contact stress between fastener and specimen is cosinusoidally distributed. Not only have these assumptions been made unnecessary, they have been shown to be invalid in certain cases.

Examination of the data in Table 1 indicates that the 3-hole specimen may yield unacceptably conservative results if used for experimental determination of load proportions in mechanical joints of the configurations examined. This result is due to the large difference in load proportioning between the fasteners.

It appears that the 5-hole specimen is somewhat representative of the response of wider specimens. Since the 5-hole specimen is less expensive to manufacture and test, it appears superior to the 7- and 9-hole specimens with regard to experimental determination of load proportioning. Through use of companion analyses using the approach reported herein, reliable results should be achieved with the 5-hole specimen.

It is believed that the capability developed during this effort and reported in this paper can now be used to predict load proportioning in multifastener joints. The methodology can be used for design of mechanically fastened joints, not only in composites, but in any material system. It is also useful in effective, systematic reduction and understanding of experimental data.

Acknowledgments

Authors Griffin, Hyer, and Yalamanchili gratefully express their appreciation for funding (PO ARIB09403 with Virginia Tech) from Hercules Aerospace Company, Inc., Bacchus Works. Thanks are also due to the NASA Langley Research Center, Hampton, Virginia, Aircraft Structures Branch, for instrumenting the specimens and assisting in performance of the experiments in this cooperative effort. The initial numerical analyses were completed before the experiments, and the results could only be regarded as interesting, curious, and potentially valuable without this crucial experimental verification.

References

[1]Hyer, M. W., and Lightfoot, M. C., "Ultimate Strength of High-Load-Capacity Composite Bolted Joints," *ASTM STP 674, Composite Materials: Testing and Design (Fifth Conference)*, edited by S. W. Tsai, American Society for Testing and Materials, Philadelphia, PA, 1979, pp. 118–136.

[2]Garbo, S. P., and Ogonowski, "Effect of Variances and Manufacturing Tolerances on the Design Strength and Life of Mechanically Fastened Composite Joints," Air Force Wright Aeronautical Labs., AFWAL-TR-81-3041, Wright-Patterson Air Force Base, OH, Vols. 1–3, April 1981.

[3]Hart-Smith, L. J., "Bolted Joints in Graphite-Epoxy Composites," NASA CR-144899, June 1976.

[4]Pyner, G. R., and Matthews, F. L., "Comparison of Single- and Multi-Hole Bolted Joints in Glass Fibre Reinforced Plastic," *Journal of Composite Materials*, Vol. 13, July 1979, pp. 232–239.

[5]Godwin, E. W., Matthews, F. L., and Kilty, P. F., "Strength of Multi-Bolt Joints in GRP," *Composites*, Vol. 13, No. 3, 1982, pp. 268–272.

[6]Rowlands, R. E., Rahman, M. U., Wilkinson, T. L., and Chiang, Y. I., "Single- and Multiple-Bolted Joints in Orthotropic Materials," *Composites*, Vol. 13, No. 3, 1982, pp. 273–278.

[7]Hyer, M. W., Klang, E. C., and Cooper, D. E., "Effects of Pin Elasticity, Clearance, and Friction on the Stresses in a Pin-Loaded Orthotropic Plate," *Journal of Composite Materials*, Vol. 21, No. 5, 1987, pp. 190–206.

[8]Chang, F. K., Scott, R. A., and Springer, G. S., "Failure Strength of Nonlinearly Elastic Composite Laminates Containing a Pin-Loaded Hole," *Journal of Composite Materials*, Vol. 18, May 1984, pp. 464–477.

[9]Hyer, M. W., and Chastain, P. A., "The Effect of Bolt Load Proportioning on the Capacity of Multiple-Bolt Composite Joints," *Journal of Aircraft*, Vol. 25, No. 2, 1988, pp. 93–113.

[10]Crews, J. H., Jr., and Naik, R. A., "Bearing-Bypass Loading on Bolted Composite Joints," NASA-TM-89153, May 1987.

[11]Cohen, D., Norton, F. M., and Hodgson, M. E., "Experimental Investigation of Failure Modes and Failure Loads in Thick Composite Joints," *Proceedings of the Fourth Technical Conference of the American Society for Composites*, Blacksburg, VA, Oct. 1989, pp. 72–81.

[12]Anon., ABAQUS, Version 4.8, copyright Hibbitt, Karlsson, and Sorensen, Inc., Pawtucket, RI, 1989.

[13]Yalamanchili, S. R., Hyer, M. W., Griffin, O. H., Jr., Shuart, M. J., Prasad, C. B., and Cohen, D., "Analysis of MultiFastener Composite Joints: Numerical and Experimental Results," Virginia Polytechnic Inst. and State Univ. College of Engineering Rept. VPI-E-92-14 (CCMS-92-15), Blacksburg, VA, June 1992.

Earl A. Thornton
Associate Editor